Published in final edited form as:
Eur Radiol. 2014 February ; 24(2): 512–518. doi:10.1007/s00330-013-3040-6.

Accuracy of Dual-Energy Computed Tomography for the Measurement of Iodine Concentration Using Cardiac CT Protocols: Validation in a Phantom Model

James D. Koonce[1], **Rozemarijn Vliegenthart**[1,2], **U. Joseph Schoepf**[1,3], **Bernhard Schmidt**[4], **Amy E. Wahlquist**[5], **Paul J. Nietert**[5], **Gorka Bastarrika**[6], **Thomas G. Flohr**[4], and **Felix G. Meinel**[1,7]

[1]Department of Radiology and Radiological Science, Medical University of South Carolina [2]Center for Medical Imaging - North East Netherlands, Department of Radiology, University of Groningen, University Medical Center Groningen, Groningen, The Netherlands [3]Department of Medicine, Division of Cardiology, Medical University of South Carolina, Charleston, SC, USA [4]Imaging & Therapy Division, Siemens Healthcare, Forchheim, Germany [5]Department of Public Health Services, Medical University of South Carolina, Charleston, SC, USA [6]Department of Radiology, University of Navarra, Pamplona, Spain [7]Institute for Clinical Radiology, Ludwig-Maximilians-University Hospital, Munich, Germany

Abstract

Purpose—To assess the accuracy of dual-energy CT (DECT) for the quantification of iodine concentrations in a thoracic phantom across various cardiac DECT protocols and simulated patient sizes.

Materials and methods—Experiments were performed on first- and second-generation dual-source CT (DSCT) systems in DECT mode using various cardiac DECT protocols. An anthropomorphic thoracic phantom was equipped with tubular inserts containing known iodine concentrations (0–20 mg/mL) in the cardiac chamber and up to two fat-equivalent rings to simulate different patient sizes. DECT-derived iodine concentrations were measured using dedicated software and compared to true concentrations. General linear regression models were used to identify predictors of measurement accuracy

Results—Correlation between measured and true iodine concentrations (n=72) across CT systems and protocols was excellent (R=0.994–0.997, P< 0.0001). Mean measurement errors were 3.0 ± 7.0 % and −2.9 ± 3.8 % for first- and second-generation DSCT, respectively. This error increased with simulated patient size. The second-generation DSCT showed the most stable measurements across a wide range of iodine concentrations and simulated patient sizes.

Corresponding Author: U. J. Schoepf, Department of Radiology and Radiological Science, Medical University of South Carolina, Ashley River Tower, 25 Courtenay Drive, Charleston, SC 29425-2260, USA, schoepf@musc.edu.

The other authors have no potential conflicts of interest to disclose.

Conclusion—Overall, DECT provides accurate measurements of iodine concentrations across cardiac CT protocols, strengthening the case for DECT-derived blood volume estimates as a surrogate of myocardial blood supply.

Keywords

dual-energy CT; dual-source CT; cardiac CT; iodine; quantification

INTRODUCTION

The first attempts to use spectral information from computed tomography (CT) data acquired at two different energies to characterize different materials were performed in the 1970s and 1980s [1,2]. Technical shortcomings prevented application of dual-energy technology in the realm of clinical medicine, but the majority of these have been overcome with the advent of dual-source CT (DSCT) systems in 2006 [1]. Iodine, commonly used as CT contrast material, shows a characteristic CT attenuation spectrum with high attenuation at low photon energies [2]. This allows differentiation from other materials and allows mapping tissue iodine distribution as a surrogate for tissue perfusion. Dual-energy CT (DECT) has recently shown capability for mapping the iodine distribution within the myocardium at a specified time point during the first pass of a contrast bolus through the left ventricle [3–6]. This iodine distribution map can be used as a surrogate for evaluating myocardial blood supply instead of dynamic, time-resolved perfusion imaging [7].

Most studies on cardiac DECT performed to date have been limited to a subjective visual evaluation of DECT iodine maps for the presence of myocardial contrast defects as signs of ischaemia or infarction and have not used quantitative measurements of myocardial iodine [3; 4; 6]. If myocardial iodine concentration can be accurately measured based on DECT-derived measurements, this might allow for quantification of myocardial perfusion on static, single-phase DECT imaging and the definition of specific iodine concentration cut-offs for normal and abnormal perfusion. In patients with coronary artery disease undergoing rest and stress DECT, this may also allow one to estimate myocardial flow reserve.

The accuracy of such estimations of myocardial perfusion depends on how accurately cardiac DECT quantifies iodine concentrations, which has not been investigated to date. Therefore, the aim of this study was to assess the accuracy of first- and second-generation DSCT systems for quantifying iodine concentration in a thoracic phantom model using various cardiac DECT acquisition protocols across a range of simulated patient sizes.

MATERIALS AND METHODS

Phantom setup

A cardiac CT phantom (Cardio CT Phantom; QRM, Forchheim, Germany) was imaged. This anthropomorphic phantom resembles a thorax, with artificial lungs and a spine insert surrounded by soft-tissue–equivalent material and a chamber in the position of the heart. The phantom is depicted in Fig. 1a. Five 50-mL syringes were filled with solutions prepared by diluting iodine contrast medium (Omnipaque 350, GE Healthcare, Princeton, USA) with

water to predetermined concentrations of 0, 5, 10, 15 and 20 mg iodine per mL. The syringes were positioned in the central cardiac chamber and held in place by a foam insert. Fig. 1b shows axial CT images of the iodine syringes. The phantom was fitted with up to two different external fat-equivalent rings to simulate larger patient sizes (F_0 = no fat ring, lateral diameter of the phantom 30 cm; F_1 = small fat ring, 5 cm, lateral diameter of the phantom 35 cm; F_2 = large fat ring, 10 cm, lateral diameter of the phantom 40 cm).

DECT Acquisition parameters

Experiments were carried out using first- and second-generation DSCT systems (Somatom Definition and Somatom Definition Flash, Siemens Healthcare, Forchheim, Germany) in dual-energy mode. For both CT systems and all CT protocols, 140kVp was the high-energy tube spectrum. For both CT systems, the mean energy of the 80 kVp, 100kVp, 140 kVp and Sn 140 kVp spectra behind the bow-tie filter at its centre were 52 keV, 58keV, 69 keV and 89 keV, respectively.

Variable first-generation DSCT acquisition parameters included acquisition mode (spiral or sequential), low-energy tube level (80 kVp or 100 kVp), and reconstruction algorithm (180° [half] or 360° [full]). The 180° reconstruction algorithm involves data from only one-half of a rotation of the CT tubes, whereas the 360° reconstruction algorithm utilizes data from a full rotation of the CT tubes. With the evaluated CT system, sequential evaluation is only feasible with the 360° rotation reconstruction algorithm. Changing these CT acquisition variables allowed for six different CT protocol combinations (Table 1). All first-generation DSCT acquisitions were obtained with the following parameters: 330 ms gantry rotation (rot) time, pitch of 0.2 in spiral modes, detector collimation 2×32×0.6 mm, slice acquisition 2×64×0.6 mm with z-flying focal spot technique. One tube of the dual-source CT system was operated with 150 mAs/rot at 140 kVp, the second tube with 165 mAs/rot at 80 kVp or 100 kVp. Automated tube current modulation was not used.

Variable second-generation DSCT acquisition parameters also included spiral and sequential acquisition mode as well as 180° and 360° reconstruction algorithms. Varying the low energy spectrum was not an option in case of second-generation DSCT; all evaluations were done with low-energy tube output at 100kVp. By using a flying z-spot technique, the second-generation DSCT can be operated in 64- or 128-slice mode. A tin filter was used in conjunction with the high energy (140 kVp) tube for all second-generation DSCT protocols to improve spectral separation. Again, sequential evaluation was only feasible with the 360° rotation reconstruction algorithm. The second-generation DECT acquisition variables also allowed six different protocol combinations. (Table 2) Second-generation DSCT parameters were as follows: 280 ms gantry rotation time, pitch of 0.17 for spiral modes, collimation 2×64×0.6 mm / 2×128×0.6 mm by means of a z-flying focal spot, tube current time 150 mAs/rot at Sn140 kVp and 165 mAs/rot at 100 kVp. Automated tube current modulation was not used.

Image Reconstruction and Analysis

All image data sets were reconstructed with 1mm slice thickness and 0.75mm increment, using a D30 dual energy cardiac kernel. The reconstructed image data sets were evaluated

on a dedicated analysis platform (Syngo-Multi-Modality Workplace, Siemens Healthcare, Forchheim, Germany) using their Perfused Blood Volume (PBV) software for material decomposition and iodine quantification. The first step in the analysis was processing of the data with parameters optimized for iodine detection in our phantom (Fig. 2a). A region of interest (ROI) with a standardized size of 100 mm^2 was then placed centrally in each of the five phantom inserts to measure the iodine concentration. (Fig. 2b) In total, 90 measurements were performed for each CT system to measure five iodine concentrations at six protocol combinations and three body sizes.

Statistical Analysis

The primary study outcome measure was an estimate of measurement error calculated for each concentration using the values measured by PBV software and the known true concentrations of iodine. The measurement error was calculated as follows:

$$\text{Measurement error}(\%)=\frac{(\text{measured iodine concentration}-\text{true iodine concention})}{\text{true iodine concentration}}$$

Because the water-filled syringes without iodine were measured as 0 mg/mL by the PBV software in each scenario, the 0 mg/mL syringe was regarded as the control measurement and was not included in the statistical analysis of factors influencing measurement accuracy.

All analyses were performed separately for first-and second-generation DSCT because each CT system used slightly different acquisition parameters. Pearson's correlation coefficient was calculated for the correlation between measured and true iodine concentration. General linear regression modelling was used to determine whether the measurement error was significantly affected by the number of fat rings, reconstruction algorithm, acquisition mode, slice number, tube spectrum and the magnitude of the true concentrations. The true concentrations were included as covariates in each of the models because higher concentrations are likely to improve relative accuracy [8]. All possible two-way interactions were individually examined and added to the model one at a time using a forward stepwise model selection approach. The final model was forced to have only significant interactions as well as all main effects of interest. SAS software (version 9.3, SAS Institute Inc., Cary, USA) was used for statistical analyses. A *P*-value of less than 0.05 was considered statistically significant.

RESULTS

First-generation DSCT

Measured and true iodine concentrations showed a strong correlation over all first-generation DSCT protocols ($r = 0.994$, $P < 0.0001$). On average, first-generation DSCT overestimated the iodine concentration by 3.0 ± 7.0 %. The accuracy of first-generation DSCT differed depending on the true concentration with 8.5 ± 9.3 % (0.4 ± 0.5 mg/mL) overestimation for 5 mg/mL iodine, 4.1 ± 4.9 % (0.4 ± 0.5 mg/mL) overestimation for 10 mg/mL, 0.1 ± 4.9 % (0.1 ± 0.5 mg/mL) overestimation for 15 mg/mL, and 0.7 ± 3.1 % (0.1 ± 0.6 mg/mL) underestimation for 20 mg/mL (Fig. 3a). There was a significant interaction

between true iodine concentration and phantom size (*P*=0.002). Measurement accuracy decreased with increasing phantom size with mean errors of −0.8 ± 3.9% without fat ring, 2.0 ± 4.9 % for the 5cm fat ring and 7.9 ± 8.3 % for the 10 cm fat ring.

The choice of the low-energy tube spectrum showed a significant interaction with true iodine concentration (*P*=0.04). Overall, accuracy of iodine measurements was better for 100kVp than for 80kVp, especially at lower iodine concentrations. This was particularly true for the large phantom size (10cm fat ring), for which the 80 kVp setting showed over three times more overestimation compared to 100 kVp. Other significant interactions included phantom size by acquisition mode (spiral vs. sequential) (*P*=0.002) and phantom size by low-energy tube output (*P*=0.0003). On average, the overestimation was 2.2 % less for full reconstruction as compared to half reconstruction (*P*=0.02).

Second-generation DSCT

A strong correlation was found between measured and true iodine concentrations over all second-generation DSCT protocols ($r = 0.997$, $P < 0.0001$). Overall, the iodine concentration was underestimated by an average of 2.9 ± 3.8 % by second-generation DSCT. The measurement error varied with the true iodine concentration, with 2.1 ± 5.0 % (0.1 ± 0.3 mg/mL) underestimation for 5 mg/mL concentration, 0.3 ± 2.9 % (0.0 ± 0.3 mg/mL) underestimation for 10 mg/mL, 4.2 ± 2.8 % (0.6 ± 0.4 mg/mL) underestimation for 15 mg/mL, and 4.9 ± 2.3 % (1.0 ± 0.5 mg/mL) underestimation for 20 mg/mL (Fig. 3b). The mean error by phantom size was 0.2 ± 3.1% without fat ring, −4.0 ± 2.4 % with the 5cm fat ring and −4.9% ± 3.7% with the 10 cm fat ring.

There were significant interactions between iodine concentration and phantom size as well as the choice of 64- or 128-slice mode (*P*<0.01). As phantom size increased, the 64-slice mode showed less underestimation than the 128-slice mode. Reconstruction method (180°; 360°) and acquisition mode (spiral vs. sequential) were not significantly related to the measurement error.

DISCUSSION

In this study we evaluated the accuracy of iodine quantification in cardiac DECT using a phantom model. We demonstrated that the overall accuracy of iodine measurements using first- and second-generation DSCT in DECT image acquisition mode is very high among all protocols that are typically applied in cardiac imaging.

The small differences in accuracy between protocols can be explained by technical considerations. At 100 kVp, more radiation dose is available than at 80 kVp, if the same mAs is used as in our study. This leads to less image noise in particular for larger patient sizes and therefore to lower variability at 100 kVp. The decreased accuracy for first-generation DSCT protocols using 80 kVp particularly for larger phantom sizes is a consequence. In a clinical setting, in which the iodine concentrations are likely less than 10 mg/mL and a considerable proportion of the patients are obese, the low-energy tube spectrum should therefore likely be set to 100kVp for first-generation DSCT cardiac CT.

Full reconstructions obtain twice as many data in the same area compared to half reconstructions, and – owing to their 360° symmetry - they are less sensitive to scattering and other artefacts caused by variable start angles. This is the likely explanation for our finding of an improved accuracy with full reconstructions on first-generation DECT systems. It should be noted that temporal resolution is reduced and the radiation dose is increased when using 360° reconstructions. These disadvantages may outweigh the 2 % gain in accuracy in a clinical setting. Overall, the accuracy of cardiac DECT was very high in our study across the different protocols with varying radiation dose levels. This suggests that image noise does not represent a major challenge for the accuracy of iodine quantification in the dose range commonly applied in cardiac CT protocols. We conclude that cardiac DECT should be performed with the lowest reasonably achievable radiation dose for each individual patient even if quantification of myocardial iodine content is desired.

As expected, there was an overall decrease of accuracy in the iodine measurements when more fat equivalent rings were added to simulate obese patients. Again, this is easily explained by noise due to photon starvation. One of our findings was that the second-generation DECT in 64 slice mode showed slightly better accuracy compared to the 128 slice mode. This may be caused by a smaller amount of cross-scatter with smaller detector width in the z-direction.

The second-generation DSCT is equipped with an additional tin filter which hardens the high-energy spectrum (then denoted as Sn140 kVp). This filter absorbs the low-energy photons thus reducing radiation dose and decreasing the spectral overlap between low- and high-energy spectra. The latter has been shown to allow for a more accurate material decomposition [9; 10] which is likely to translate into more accurate iodine quantification. This agrees well with our findings of overall slightly improved iodine measurement accuracy with second-generation DSCT compared to the first-generation DSCT.

A previous study on dual-energy CT of the chest has found a higher contrast-to-noise ratio using the first-generation 140/80 kVp mode compared to the second-generation Sn140/100 kVp protocol [11]. Nevertheless, we found a better accuracy for the Sn140/100 kVp protocol for iodine quantification. The most plausible interpretation of these data is that the decreased spectral overlap with the tin filtrated 140 kVp spectrum allows for a more accurate material decomposition despite an equal or lower contrast-to-noise ratio. Additionally, the apparent discrepancy can be explained by differences in study design, as the previous study used a relatively slim Alderson phantom and did not vary phantom size or iodine concentrations. This is important since the advantage of the second-generation Sn140/100 kVp protocol in our study was most pronounced for large phantom sizes and low iodine concentrations.

DECT offers the potential to assess coronary integrity, cardiac morphology and myocardial perfusion in a single comprehensive imaging exam. The qualitative visual analysis of myocardial iodine distribution maps derived from DECT has been validated in animal models [12] and has already shown promise for the evaluation of myocardial perfusion defects associated with coronary artery disease in a clinical setting [3–6; 13–16]. An incremental value of dual-energy over single-energy CT has been found for the visual evaluation of myocardial perfusion on first-pass CT [17]. Compared with single-energy

first-pass perfusion CT, DECT allows not only for a visual analysis of myocardial contrast enhancement but also for a direct quantification of myocardial blood content [18].

In other clinical applications, the quantification of tissue iodine content has been applied with great success. Multiple studies have shown that iodine enhancement on dual-energy CT can reliably differentiate enhancing renal neoplasms from benign high attenuation cysts [19–21]. In oncological imaging, the quantification of iodine has been used for the characterization of masses and for the assessment of therapy response [22]. The quantification of pulmonary iodine content has been shown to indicate the severity of pulmonary disorders including emphysema [23] and pulmonary embolism [24].

Similarly, the quantification of myocardial iodine content is likely to play an increasing role in dual-energy cardiac CT. Our study demonstrates very good overall accuracy for the quantification of iodine in cardiac DSCT protocols. This is an important step towards studying the diagnostic and prognostic value of objective quantitative myocardial iodine measurements in a clinical setting.

The results of our study need to be seen in the context of the study design and its limitations. Firstly, measuring concentration in a phantom is inherently different than evaluating patients. The phantom is a completely static object, and variability caused by breathing, myocardial contraction and other movement does not impact outcome as would be the case in a clinical setting. However, our results are important because we investigated the accuracy of iodine measurements under controlled circumstances thus providing the rationale for applying the technique in a clinical setting. A second limitation is that the difference between solutions increased at 5 mg/mL increments between each syringe. In our own experience, iodine concentrations in healthy myocardium at contrast-enhanced first-pass CT typically fall in the range of 3–8 mg/mL. Further studies may evaluate DECT iodine concentration measurements with lower concentrations and more subtle differences in concentrations. Thirdly, we limited our study to DSCT because this was the only DECT technique used for myocardial perfusion assessment when we initiated the study. Recently, the feasibility of dual-energy myocardial perfusion CT using rapid kV switching has been demonstrated [15]. Our data may not be valid for this technique.

In conclusion, DECT provides accurate measurements of iodine concentration using cardiac acquisition protocols and different simulated patient sizes. The second-generation DSCT system showed the most stable measurements across a wide range of iodine concentrations and simulated patient sizes. Our data provide the rationale for clinical studies on the quantification of myocardial iodine content in dual-energy CT to assess regional myocardial perfusion abnormalities.

Acknowledgments

Dr. Schoepf is a consultant for and receives research support from Bayer, Bracco, GE, Medrad, and Siemens. Dr. Schmidt and Dr. Flohr are Siemens employees.

The project described was supported by Award Number UL1TR000062 from the National Center for Research Resources. The content is solely the responsibility of the authors and does not necessarily represent the official views of the National Center for Research Resources or the National Institutes of Health.

Abbreviations

DECT	Dual-energy computed tomography
DSCT	Dual-source computed tomography
ROI	Region of interest

REFERENCES

1. Flohr TG, McCollough CH, Bruder H, et al. First performance evaluation of a dualsource CT (DSCT) system. Eur Radiol. 2006; 16:256–268. [PubMed: 16341833]
2. Johnson TR, Krauss B, Sedlmair M, et al. Material differentiation by dual energy CT: initial experience. Eur Radiol. 2007; 17:1510–1517. [PubMed: 17151859]
3. Ko SM, Choi JW, Song MG, et al. Myocardial perfusion imaging using adenosineinduced stress dual-energy computed tomography of the heart: comparison with cardiac magnetic resonance imaging and conventional coronary angiography. Eur Radiol. 2011; 21:26–35. [PubMed: 20658242]
4. Ruzsics B, Lee H, Zwerner PL, Gebregziabher M, Costello P, Schoepf UJ. Dual-energy CT of the heart for diagnosing coronary artery stenosis and myocardial ischemia-initial experience. Eur Radiol. 2008; 18:2414–2424. [PubMed: 18523782]
5. Schwarz F, Ruzsics B, Schoepf UJ, et al. Dual-energy CT of the heart--principles and protocols. Eur J Radiol. 2008; 68:423–433. [PubMed: 19008064]
6. Wang R, Yu W, Wang Y, et al. Incremental value of dual-energy CT to coronary CT angiography for the detection of significant coronary stenosis: comparison with quantitative coronary angiography and single photon emission computed tomography. Int J Cardiovasc Imaging. 2011; 27:647–656. [PubMed: 21547377]
7. Vliegenthart R, Henzler T, Moscariello A, et al. CT of coronary heart disease: Part 1, CT of myocardial infarction, ischemia, and viability. AJR Am J Roentgenol. 2012; 198:531–547. [PubMed: 22357992]
8. Ravenel JG, Leue WM, Nietert PJ, Miller JV, Taylor KK, Silvestri GA. Pulmonary nodule volume: effects of reconstruction parameters on automated measurements--a phantom study. Radiology. 2008; 247:400–408. [PubMed: 18430874]
9. Primak AN, Ramirez Giraldo JC, Liu X, Yu L, McCollough CH. Improved dual-energy material discrimination for dual-source CT by means of additional spectral filtration. Med Phys. 2009; 36:1359–1369. [PubMed: 19472643]
10. Karlo C, Lauber A, Gotti RP, et al. Dual-energy CT with tin filter technology for the discrimination of renal lesion proxies containing blood, protein, and contrast-agent. An experimental phantom study. Eur Radiol. 2011; 21:385–392. [PubMed: 20711733]
11. Schenzle JC, Sommer WH, Neumaier K, et al. Dual energy CT of the chest: how about the dose? Invest Radiol. 2010; 45:347–353. [PubMed: 20404737]
12. Zhang LJ, Peng J, Wu SY, Yeh BM, Zhou CS, Lu GM. Dual source dual-energy computed tomography of acute myocardial infarction: correlation with histopathologic findings in a canine model. Invest Radiol. 2010; 45:290–297. [PubMed: 20421797]
13. Vliegenthart R, Pelgrim GJ, Ebersberger U, Rowe GW, Oudkerk M, Schoepf UJ. Dualenergy CT of the heart. AJR Am J Roentgenol. 2012; 199:S54–S63. [PubMed: 23097168]
14. Ruzsics B, Schwarz F, Schoepf UJ, et al. Comparison of dual-energy computed tomography of the heart with single photon emission computed tomography for assessment of coronary artery stenosis and of the myocardial blood supply. Am J Cardiol. 2009; 104:318–326. [PubMed: 19616661]
15. So A, Hsieh J, Imai Y, et al. Prospectively ECG-triggered rapid kV-switching dualenergy CT for quantitative imaging of myocardial perfusion. JACC Cardiovasc Imaging. 2012; 5:829–836. [PubMed: 22897997]
16. Ko SM, Choi JW, Hwang HK, Song MG, Shin JK, Chee HK. Diagnostic performance of combined noninvasive anatomic and functional assessment with dual-source CT and adenosine-induced

stress dual-energy CT for detection of significant coronary stenosis. AJR Am J Roentgenol. 2012; 198:512–520. [PubMed: 22357990]

17. Arnoldi E, Lee YS, Ruzsics B, et al. CT detection of myocardial blood volume deficits: dual-energy CT compared with single-energy CT spectra. J Cardiovasc Comput Tomogr. 2011; 5:421–429. [PubMed: 22146501]
18. Hoffmann U, Truong QA, Schoenfeld DA, et al. Coronary CT angiography versus standard evaluation in acute chest pain. N Engl J Med. 2012; 367:299–308. [PubMed: 22830462]
19. Graser A, Becker CR, Staehler M, et al. Single-phase dual-energy CT allows for characterization of renal masses as benign or malignant. Invest Radiol. 2010; 45:399–405. [PubMed: 20498609]
20. Chandarana H, Megibow AJ, Cohen BA, et al. Iodine quantification with dual-energy CT: phantom study and preliminary experience with renal masses. AJR Am J Roentgenol. 2011; 196:W693–W700. [PubMed: 21606256]
21. Song KD, Kim CK, Park BK, Kim B. Utility of iodine overlay technique and virtual unenhanced images for the characterization of renal masses by dual-energy CT. AJR Am J Roentgenol. 2011; 197:W1076–W1082. [PubMed: 22109322]
22. De Cecco CN, Darnell A, Rengo M, et al. Dual-energy CT: oncologic applications. AJR Am J Roentgenol. 2012; 199:S98–S105. [PubMed: 23097174]
23. Meinel FG, Graef A, Thieme SF, et al. Assessing pulmonary perfusion in emphysema: automated quantification of perfused blood volume in dual-energy CTPA. Invest Radiol. 2013; 48:79–85. [PubMed: 23288014]
24. Meinel FG, Graef A, Bamberg F, et al. Effectiveness of Automated Quantification of Pulmonary Perfused Blood Volume Using Dual-Energy CTPA for the Severity Assessment of Acute Pulmonary Embolism. Invest Radiol. 2013

Key points

1. Dual-energy CT provides new opportunities for quantitative assessment in cardiac imaging.
2. DECT can quantify myocardial iodine as a surrogate for myocardial perfusion.
3. DECT measurements of iodine concentrations are overall very accurate.
4. The accuracy of such measurements decreases as patient size increases.

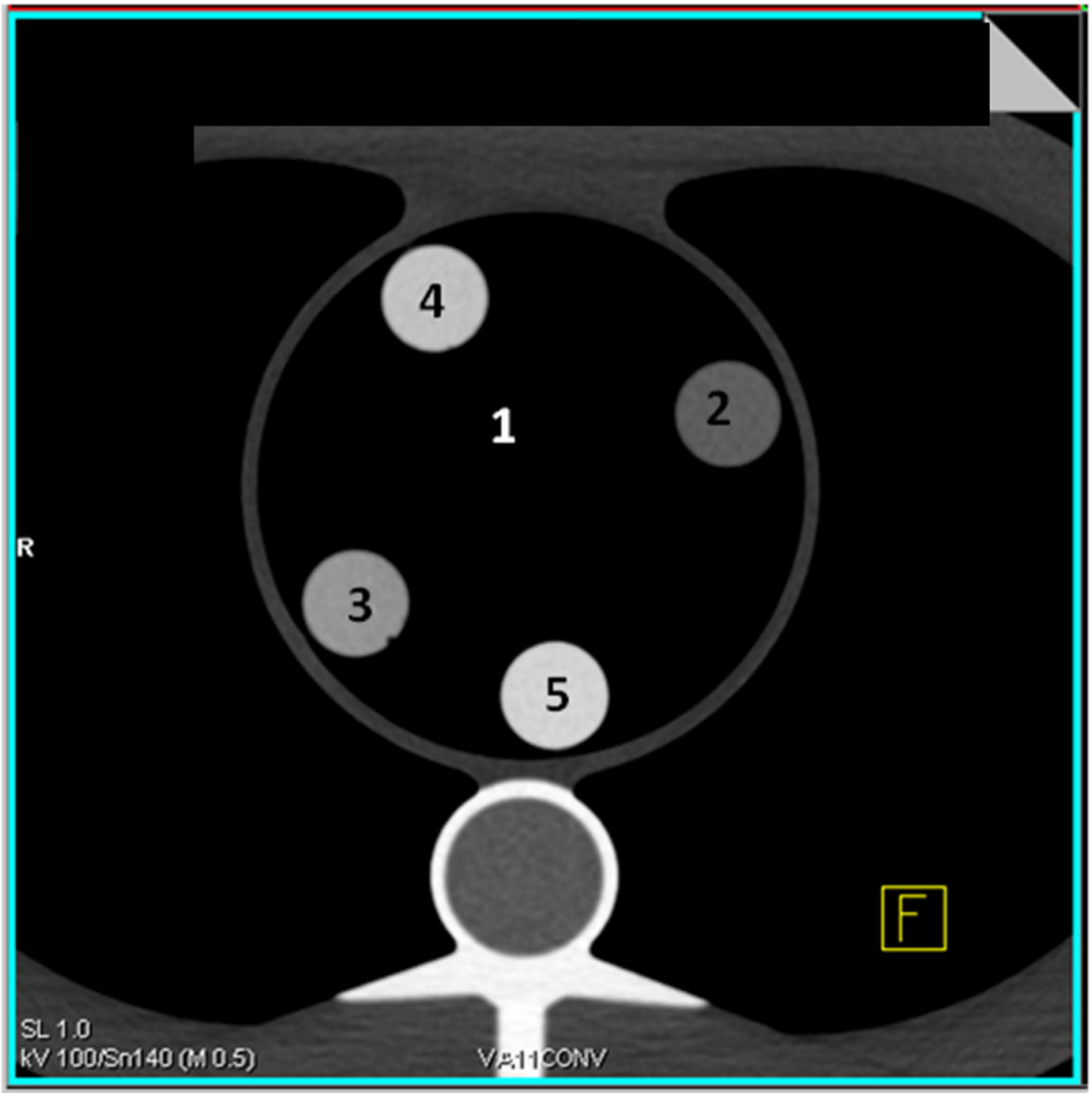

Fig. 1. Phantom setup

A, The anthropomorphic thoracic phantom is shown without iodine inserts in the central chamber. **B**, Representative axial CT images of the phantom with iodine syringes in the central chamber are shown. Syringes are labelled as follows: 1) 0 mg/mL iodine, 2) 5 mg/mL iodine, 3) 10 mg/mL iodine, 4) 15 mg/mL iodine, and 5) 20 mg/mL iodine.

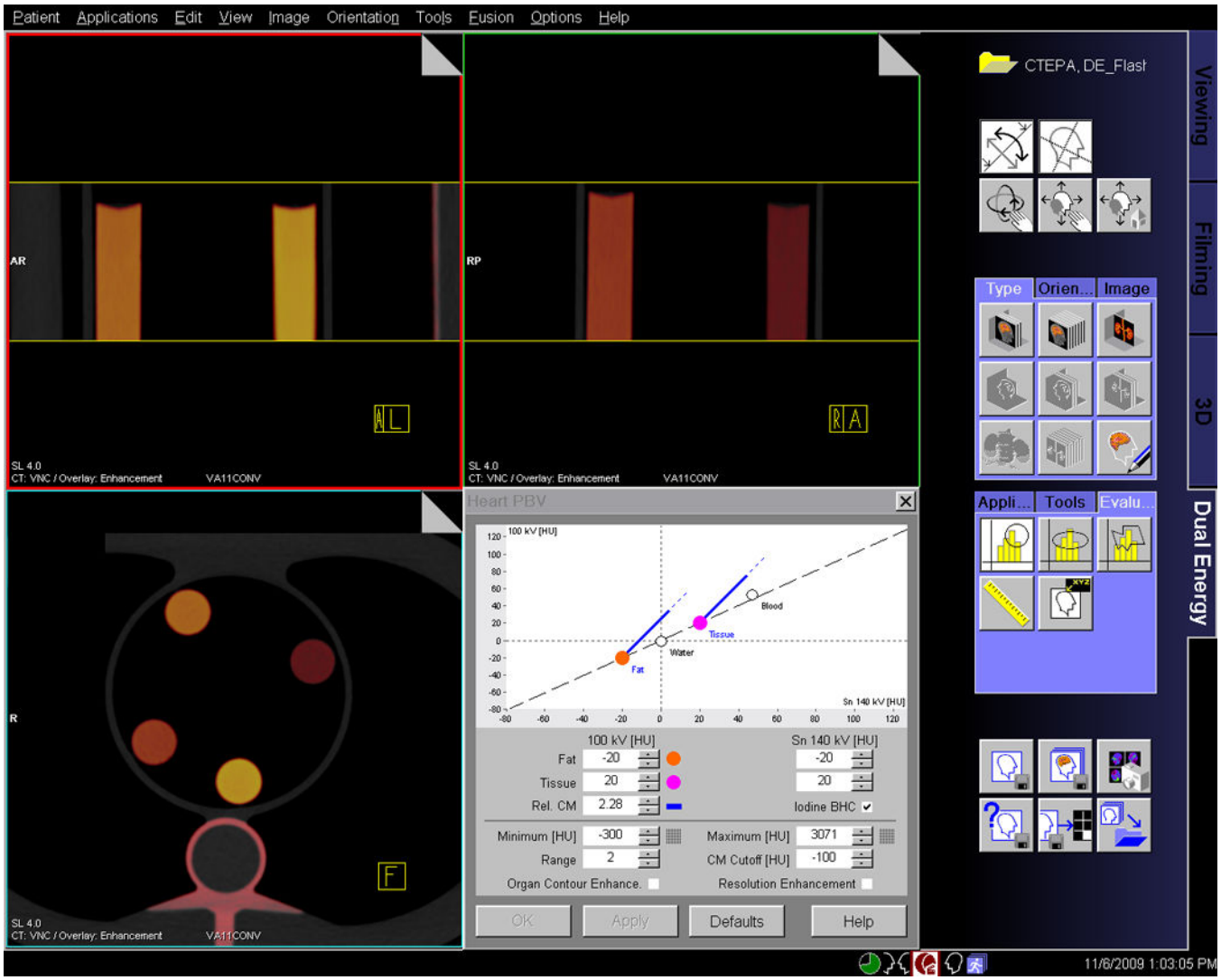

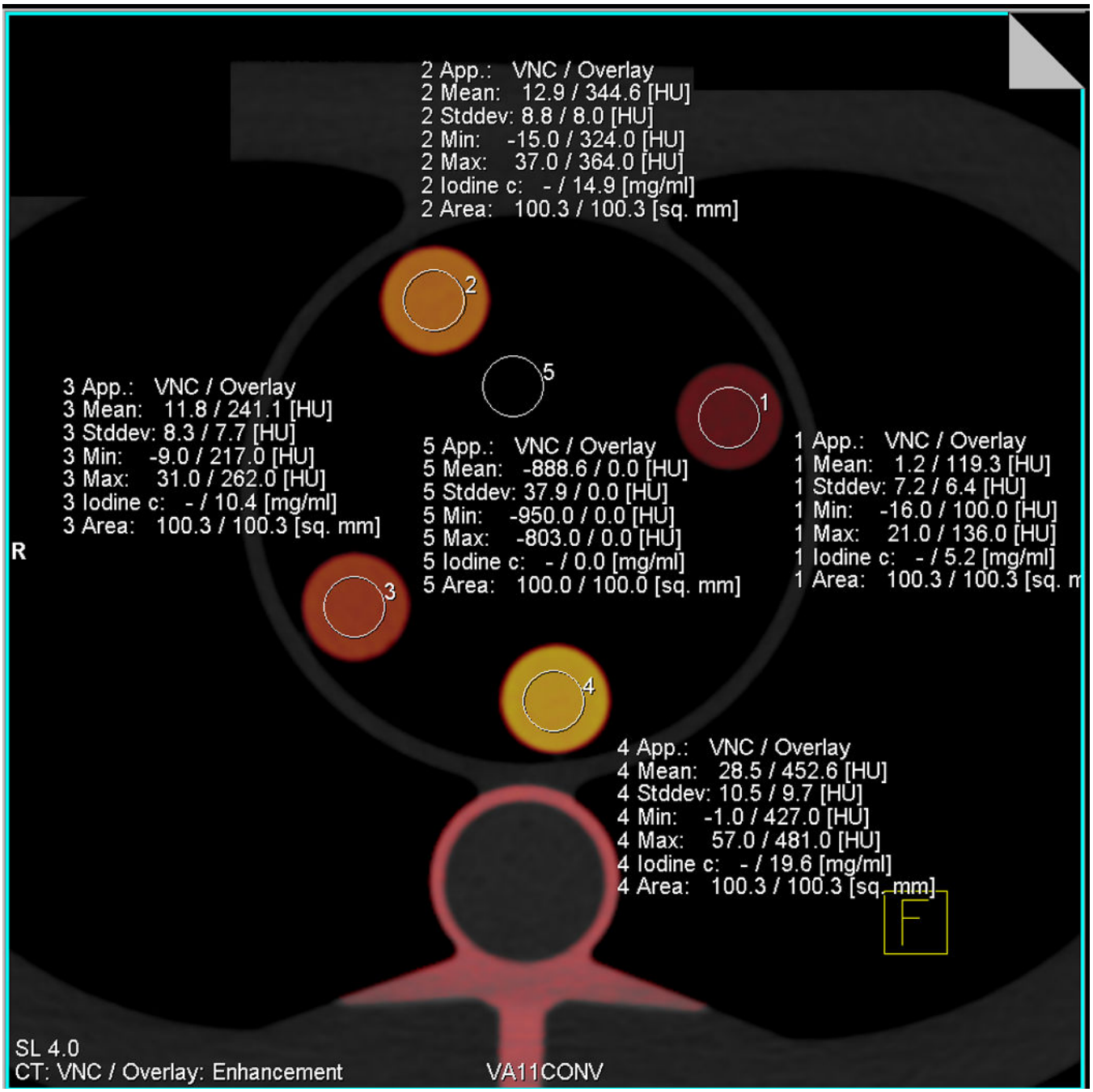

Fig. 2. Principle of iodine concentration measurements in dual-energy CT

A, This screenshot from the dual-energy analysis software demonstrates the colour-coded representation of different iodine concentration. The standard parameters used for three-material decomposition and iodine quantification are seen in the right lower corner. **B**, This screenshot illustrates the measurement of iodine content by placing standardized circular regions of interest in the inserts. The software directly displays iodine concentration in mg/mL.

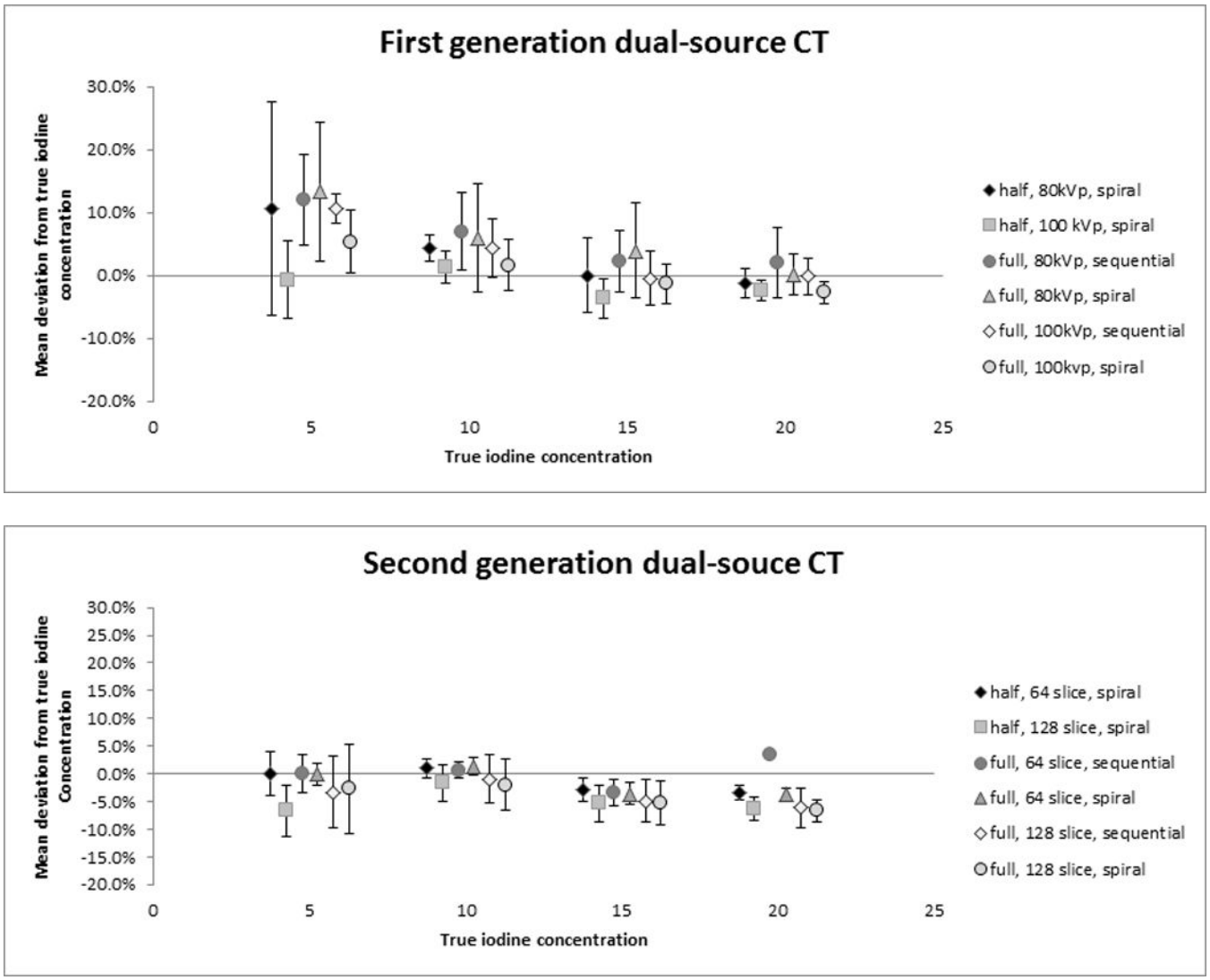

Fig. 3. Accuracy of cardiac dual-source CT for the quantification of iodine concentrations

The plots demonstrate the mean relative error in the quantification of iodine concentrations for first-generation **(A)** and second-generation DSCT **(B)**. The symbols represent the mean measurement error over all three phantom sizes with the standard deviation shown as whiskers.

Table 1

Acquisition Protocols in First-Generation Dual-Source CT

	Acquisition mode	Low-energy spectrum	Reconstruction mode
1	Sequential	80 kVp	360 degree (full)
2	Sequential	100 kVp	360 degree (full)
3	Spiral	80 kVp	360 degree (full)
4	Spiral	100 kVp	360 degree (full)
5	Spiral	80 kVp	180 degree (half)
6	Spiral	100 kVp	180 degree (half)

Table 2

Acquisition Protocols in Second-Generation Dual-Source CT

	Acquisition Mode	64 / 128 slice mode	Reconstruction Mode
1	Sequential	64	360 degree (full)
2	Sequential	128	360 degree (full)
3	Spiral	64	360 degree (full)
4	Spiral	128	360 degree (full)
5	Spiral	64	180 degree (half)
6	Spiral	128	180 degree (half)